A Phosphorus-Containing Diamine for Flame-Retardant, High-Functionality Epoxy Resins. I. Synthesis, Reactivity, and Thermal Degradation Properties

Weichang Liu,[1] Russell J. Varley,[2] George P. Simon[1]

[1]*School of Physics and Materials Engineering, Monash University, Clayton, Victoria, 3800, Australia*
[2]*CSIRO Molecular Science, Clayton, Victoria, 3168, Australia*

Received 26 June 2003; accepted 1 December 2003

ABSTRACT: A phosphorus-containing amine, bis(4-aminophenoxy)phenyl phosphine oxide (BAPP), suitable for curing epoxy resins with improved fire performance was synthesized and characterized with Fourier transform infrared spectroscopy and nuclear magnetic resonance. The reactivity of the amino group was evaluated by differential scanning calorimetry of the epoxy–amine mixture and by proton nuclear magnetic resonance of the amino unit. With BAPP as a curing agent, a range of high-functionality, aerospace epoxy resins were cured, and the dynamic kinetic parameters calculated from Kissinger's and Ozawa's models were compared with those from the more widely used amines. The thermal degradation properties of the phosphorus-containing epoxy resins were studied by thermogravimetric analysis, the degradation activation energy was calculated, and a multistep thermal degradation process was observed. © 2004 Wiley Periodicals, Inc. J Appl Polym Sci 92: 2093–2100, 2004

Key words: resins; flame retardance; kinetics (polym.)

INTRODUCTION

Epoxy resins are among the most widely used products for coatings, adhesives, encapsulating materials, and composites. However, as with most polymeric materials, an important aspect is their flammability. There are a number of ways in which epoxy resins can be made more flame-retardant. These include inorganic flame retardants, such as aluminum trioxide, ammonium polyphosphate, and red phosphorus; halogenated flame retardants, primarily based on chlorine and bromine; organophosphorus flame retardants, mainly being phosphate esters; and nitrogen-based organic flame retardants. The combination of different types of these flame retardants can lead to a synergistic improvement in the fire performance property.[1–3]

Although halogenated flame retardants show good flame retardancy and have been used widely for several decades, their use has been curtailed in many countries because of the toxic and corrosive fumes released during combustion and the bioaccumulated toxic substances produced. For this reason, the development of halogen-free flame retardants is becoming important. Halogen-containing flame retardants act in a fundamentally different way than phosphorous fire retardants. Halogen additives function by chemically interfering with the free-radical reactions that occur during combustion, whereas phosphorus-containing flame retardants promote the production of a thermally stable char layer and thus prevent heat transfer.

Flame-retardant epoxy resins can be achieved through the addition of phosphorus-containing oxiranes, and a number of articles have been published in this field.[4–13] However, flame retardancy can also be imparted with phosphorus-containing curing agents.[5,9,14–20] The introduction of phosphorus via curing agents has the advantage of ensuring that a wide range of epoxy resins (including mixtures) can be used. Although bis(4-aminophenoxy)phenyl phosphine oxide (BAPP) has been synthesized,[20,21] it has only been used with commercial Epon 828, and its reactivity and curing kinetics have not yet been reported.

In this study, BAPP was synthesized and characterized by means of Fourier transform infrared (FTIR) spectrometer and nuclear magnetic resonance (NMR). The reactivity of BAPP with three commercial epoxy resins of various functionalities—diglycidyl ether of bisphenol A (DGEBA), triglycidyl *p*-amino phenol (TGAP), and tetraglycidyl dimethylenedianiline (TGDDM)—were studied by means of NMR and differential scanning calorimetry (DSC) and were compared with 4,4′-diaminodiphenyl methane (DDM) and 4,4′-diaminodiphenyl sulfone (DDS). TGAP and TGDDM are high-modulus, high-glass-transition epoxy resins widely used in prepregs in the aerospace industry, for

Correspondence to: G. P. Simon (george.simon@spme.monash.edu.au).

Journal of Applied Polymer Science, Vol. 92, 2093–2100 (2004)

which fire retardancy is likely to be very important. The dynamic curing kinetics were studied with scanning DSC and with the models of Kissinger and Ozawa. The thermal degradation behavior of the cured phosphorus-containing epoxy resins was determined with thermogravimetric analysis (TGA) for the purpose of gaining insight into the possible flame-retardant properties of the cured resins.

EXPERIMENTAL

Materials

The precursors required for synthesizing BAPP/phenylphosphonic dichloride, 4-nitrophenol, copper(I) chloride, palladium in activated carbon, and triethylamine were purchased from Aldrich and used without further purification. Tetrahydrofuran (THF) was dried and stored with 4-Å molecule sieves. Three epoxide products—DGEBA, TGAP, and TGDDM—were obtained from Vantico, the epoxide equivalent weights being 189.7, 106.3, and 105.5 g/epoxide, respectively.

Characterization

DSC was used to determine the melting points of the intermediate compound and product and the epoxy–amine reaction behavior. The measurement was carried out with a Mettler–Toledo DSC 821E under a constant flow of nitrogen (50 mL/min), the instrument being calibrated with In and Zn. The melting point was taken from the maximum of the endothermic peak at a heating rate of 10°C/min. Uncured epoxy–amine samples were ramped from 25 to 280°C at heating rates of 2.5, 5, 10, 15, and 20°C/min. The exothermic peak was identified not only by its maxima [peak temperature (T_p)] but also in terms of the temperature at which the DSC signal departed from the baseline at the low-temperature side [initial temperature (T_{ini})] and the temperature at the intersection of the extrapolation of the baseline and the extrapolation from the peak shoulder at the low-temperature side [onset temperature (T_{on})].

TGA measurements were performed with a Mettler–Toledo TGA/SDTA 851E in air and nitrogen atmospheres. In both measurements, the flow rate was set at 50 mL/min.

FTIR spectra were obtained with a Bomem MB100 infrared spectrophotometer. NMR data were measured with a Bruker AC200SX; a 10–12 mg sample was used with deuterated dimethyl sulfoxide (DMSO-d_6) as the solvent.

Synthesis of bis(4-nitrophenoxy)phenyl phosphine oxide (BNPP)

4-Nitrophenol (27.8 g, 200 mmol) and triethylamine (20.2 g, 200 mmol) were dissolved in 70 mL of THF and cooled to 0°C in an ice bath. After the addition of Cu_2Cl_2 (0.35 g), a solution of phenylphosphonic dichloride (19.5 g, 100 mmol) in 40 mL of THF was dropped into the system over a period of 2.5 h. The reaction was kept at room temperature for 24 h, and the precipitant was filtered and washed with THF. The filtrate was concentrated with a rotary vacuum dryer and poured into a saturated sodium chloride solution. The precipitant was vacuum-dried and recrystallized twice by ethanol to give 30 g of a light yellow crystal (75% yield).

FTIR (KBr disc): 1199 (P—O—Ph), 1234 (—P═O), 1346, 1518 cm^{-1} (Ph—NO_2). ^{1}H-NMR (DMSO-d_6, δ): 7.42–7.48 (double peak, aromatic protons near the NO_2 group, 4H), 7.52–8.21 (multipeak, aromatic protons in P—C_6H_5, 5H), 8.22–8.28 ppm (double peak, aromatic protons near the O—P═O group, 4H). ^{31}P-NMR (DMSO-d_6, δ): 14.00 ppm (single peak).

Synthesis of BAPP

BNPP (24 g, 60 mmol) was dissolved in 300 mL of methanol under the protection of nitrogen. After the addition of Pd/C (0.2 g) as a catalyst, the reaction system was degassed three times and was connected to hydrogen. The reaction stopped after about 8.5 L of hydrogen was consumed. The catalyst was filtered, and the solvent was removed by vacuum drying. The product was dissolved from the residue with 7*N* hydrochloric acid and was neutralized with sodium hydroxide. The resultant black solid was washed with a 0.1*N* sodium hydrogen carbonate solution and water three times. The yield was 15 g (73.5%).

FTIR (KBr disc): 3499, 3390 (Ph—NH_2), 1184 (P—O—Ph), 1255 cm^{-1} (P═O). ^{31}P-NMR (DMSO-d_6, δ): 13.55 ppm (single peak).

The ^{1}H-NMR spectrum is shown in Figure 1.

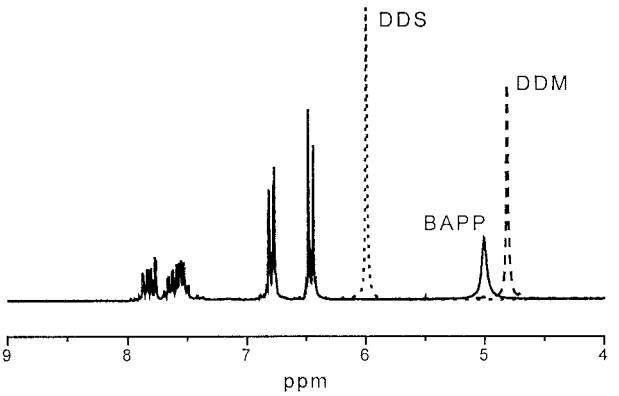

Figure 1 ^{1}H-NMR spectrum of BAPP with the chemical shifts of the amino protons in DDM and DDS.

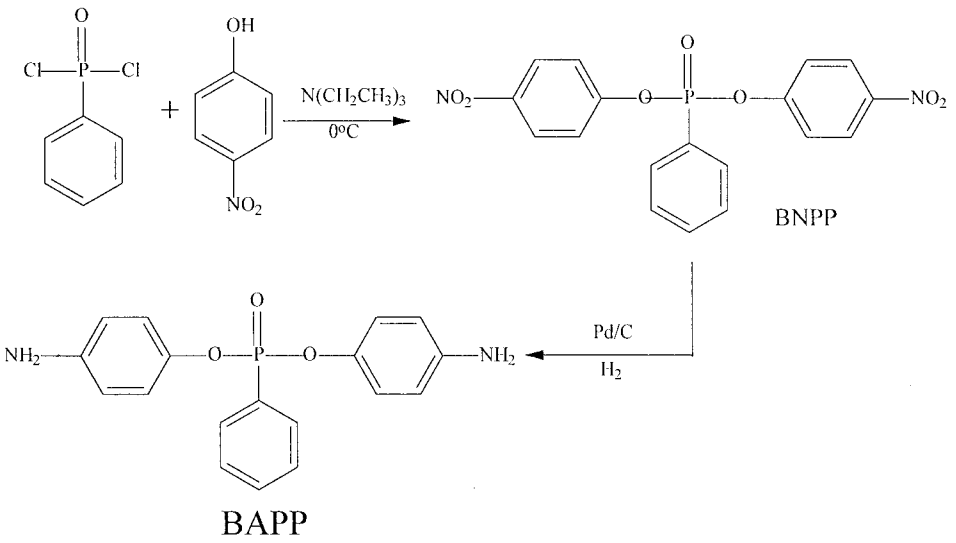

Scheme 1 Synthetic route for BAPP.

Preparation of the cured epoxy resins

DGEBA, TGAP, or TGDDM was mixed with BAPP at 80°C to yield a clear liquid. BAPP was used in a molar excess of 10%. The curing cycle was set at 100°C for 2 h, 120°C for 2 h, and 175°C for 4 h.

RESULTS AND DISCUSSION

Synthesis and characterization of BAPP

BAPP was synthesized via a two-step route shown briefly in Scheme 1. The intermediate, BNPP, had a melting point at 104.2°C, and the peaks at 1234 and 1518 cm^{-1} in the FTIR spectrum indicated the P═O and N═O groups, respectively. BAPP was produced from the reduction of BNPP and was melted at 115.2°C. The peaks at 3499 and 3390 cm^{-1} in the FTIR spectrum were attributed to the absorption of the primary amino group. ^{1}H-NMR analysis (Fig. 1) showed two peaks at 7.5–7.9 ppm that were due to the resonance of the aromatic protons in the benzene connecting directly to the phosphine oxide group; the peaks from 6.4 to 6.8 ppm were attributed to the resonance of the aromatic protons in the phenoxy group. The peak at 5.0 ppm in ^{1}H-NMR was the resonance due to the hydrogen in the amino group; the deviation from the datum reported in ref. 20 was due to the different solvent used in the NMR measurement. This peak was quenched by the addition of one drop of D_2O, which gave powerful evidence for identifying the amino group.[21] The ^{1}H-NMR spectra of DDM and DDS, two amines widely used in the aerospace epoxy industry, were also measured in DMSO-d_6 and compared with that of BAPP in Figure 1.

NMR can be used to yield important information about the reactivity of the amino group, as judged by the chemical shift. The lower the chemical shift is of the proton in the amino group, the larger pK_a is of the proton[22] and, therefore, based on the nucleophilic addition mechanism of the epoxy/primary amine reaction, the higher its reactivity is. The amino group in DDS showed the highest chemical shift at 6.0 ppm and the lowest basicity and, therefore, reactivity. The amino group in BAPP showed a slightly higher chemical shift than that of DDM; this means that phosphine oxide, an electron-withdrawing group, influences the basicity of the amine, although not to a great degree. It can be deduced that, according to this method of analysis, BAPP has a curing reactivity comparable to that of DDM but a higher reactivity than DDS. The reactivity of BAPP was further investigated with the DSC technique.

Curing process of the diamine with DGEBA, TGAP, and TGDDM

The curing behaviors of DGEBA, TGAP, and TGDDM with BAPP were studied with DSC in the dynamic scanning mode. Typical examples of DSC traces for the DGEBA/BAPP system with different ramp rates are shown in Figure 2.

The data from dynamic DSC measurements were analyzed with Kissinger's method and Ozawa's method. In Kissinger's method,[23] the reaction rate (r) is calculated as follows:

$$r = \frac{dx}{dt} = \beta\frac{dx}{dT} = Ae^{(E/RT)}(1 - x)^n \qquad (1)$$

where x is the extent of the reaction; β is the heating rate; T is the absolute temperature; t is the time; R is the gas constant; and A, E, and n are the pre-exponen-

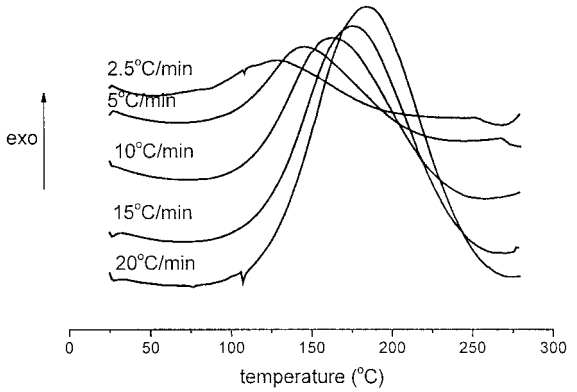

Figure 2 DSC traces of DGEBA/BAPP at different heating rates.

tial factor, the activation energy, and the order of the reaction, respectively. The maximum rate occurs at T_p, so if eq. (1) is differentiated with respect to time and equated to zero, the result is

$$\beta \frac{E}{RT_p^2} = An(1-x)_p^{n-1} e^{(-E/RT_p)} \quad (2)$$

Equation (2) can be rewritten in the natural logarithm form as

$$-\ln\left(\frac{\beta}{T_p^2}\right) = \ln\left(\frac{E}{R}\right) - \ln(An) - (n-1) \times \ln(1-x)_p + \frac{E}{RT_p} \quad (3)$$

From T_p and the heating rate, the scatter graph of $\ln(\beta/T_p^2)$ against $1/T_p$ can be drawn. The data of DGEBA/BAPP were treated, and the scatter of $\ln(\beta/T_p^2)$ versus $1/T_p$ is shown in Figure 3(a), the straight line having been drawn according to the method of least squares. The activation energy could thus be calculated from the slope of the straight line and is shown in Table I.

In Ozawa's method,[24] the relationship between the heating rate and T_p is given as

$$\log\beta = \frac{1}{2.303}\ln\beta = -0.4567\frac{E}{RT} + \log\frac{AE}{R} - \log F(x) - 2.315 \quad (4)$$

where $F(x)$ is the conversion-dependent term. Thus, for a given conversion (e.g., 50%), the relationship between ln β and $1/T_p$ should be a straight line. The scatter plot of ln β and $1/T_p$ for DGEBA/BAPP is shown in Figure 3(b), in which a linear fit has been made to the experimental data points. From the slope

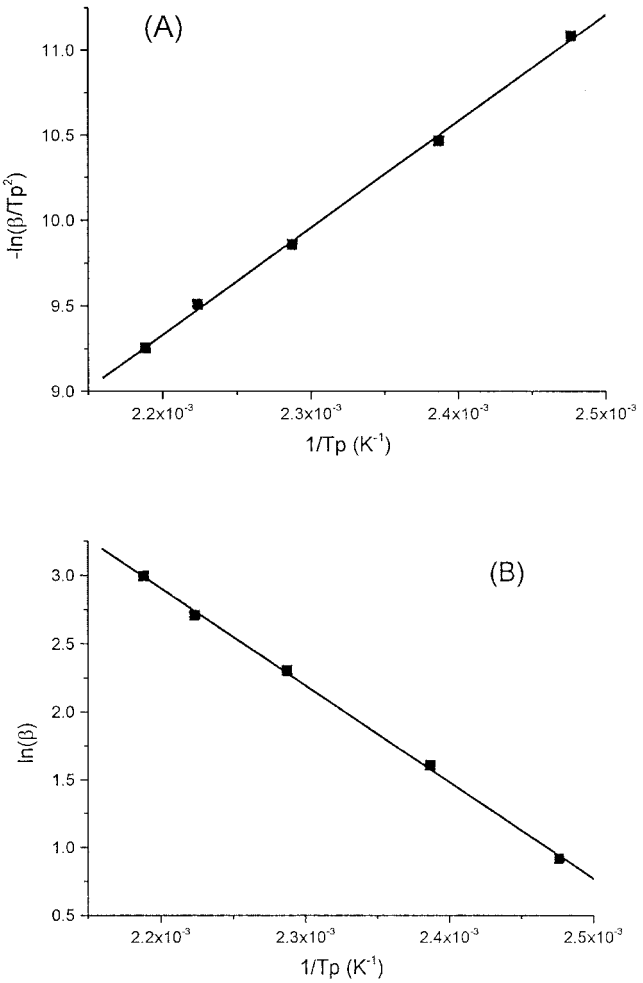

Figure 3 Dynamic kinetic analysis and calculation of the curing activation energies of DGEBA/BAPP: (A) Kissinger's method and (B) Ozawa's method.

of the straight line, the activation energy can also be calculated, and it is summarized in Table I.

BAPP has a curing activation energy comparable to that of DDM; for example, the activation energy of the DGEBA/BAPP system (52.1 ± 1.1 kJ/mol) is located within the reported range of that of DGEBA/DDM (50–59 kJ/mol).[25] However, BAPP has a lower activation energy than DDS; for example, the activation energy of the TGDDM/BAPP system (58.0 ± 0.6 kJ/mol) is much smaller than that of TGDDM/DDS (70

TABLE I
Curing Activation Energies Calculated from Dynamic DSC

System	Activation energy (kJ/mol)	
	Kissinger's method	Ozawa's method
DGEBA/BAPP	52.1 ± 1.1	56.3 ± 1.0
TGAP/BAPP	53.3 ± 1.3	57.5 ± 1.3
TGDDM/BAPP	58.0 ± 0.6	62.2 ± 0.6

TABLE II
Curing Parameters Obtained from DSC Scanning Spectra of DGEBA, TGAP, and TGDDM with BAPP

Ramp rate (°C/min)	DGEBA/BAPP			TGAP/BAPP			TGDDM/BAPP		
	T_{ini} (°C)	T_{on} (°C)	T_p (°C)	T_{ini} (°C)	T_{on} (°C)	T_p (°C)	T_{ini} (°C)	T_{on} (°C)	T_p (°C)
2.5	50.0	80.0	130.7	62.9	81.8	132.1	100.0	118.2	148.1
5	67.8	100.9	145.8	62.5	98.2	149.9	100.7	132.1	165.1
10	74.3	110.5	164.0	79.1	112.9	167.7	105.2	146.9	181.8
15	67.7	119.1	176.6	79.1	116.7	177.9	112.4	157.2	193.1
20	86.8	123.8	183.8	86.2	125.0	185.1	119.2	162.5	201.0

kJ/mol).[26] The relatively low activation energy of BAPP arises for two reasons: (1) the P—O—C linkage is flexible and the pendant phenyl group is not as bulky as those in other amines[19] and (2) the electron-withdrawing phosphine oxide group does not reduce the reactivity of amino groups significantly.

The curing behaviors of DGEBA, TGAP, and TGDDM with BAPP are summarized in Table II. Apart from T_p, T_{ini} and T_{on} are used complementarily to describe the curing behavior and to assess the reactivity of the amine. T_{ini} and T_{on}, taken from a 10°C/min scan of the DGEBA/DDM system, are 72 and 111°C, respectively,[5,12] quite similar to those of the DGEBA/BAPP system, whereas T_{on} of the DGEBA/DDS system is higher than 140°C at the same heating rate.[20] According to an analysis of T_{ini} and T_{on}, the reactivity of BAPP is comparable to that of DDM and much higher than that of DDS; this gives support to the conclusion of the ^{1}H-NMR analysis.

TGA

The thermal degradation properties of DGEBA/BAPP, TGAP/BAPP, and TGDDM/BAPP were studied with TGA, and the spectra of DGEBA/BAPP at different scanning rates are shown in Figure 4 as examples. In contrast to the single thermal degradation from 330 to 400°C of DGEBA/DDM in an atmosphere of N_2,[5] a two-step degradation of DGEBA/BAPP was found in an atmosphere of N_2. Although the weight loss of DGEBA/BAPP in nitrogen commenced at 320°C, some 10°C lower than for DGEBA/DDM, the weight-loss rate slowed after 360°C, and the char yield (31%) at 700°C was higher than that of DGEBA/DDM (20%). A more complicated thermal degradation of DGEBA/BAPP was found in an air atmosphere, whereas a clear two-step degradation was observed in air for DGEBA/DDM.[5] A high char yield of 31% at 700°C in air was found for DGEBA/BAPP, whereas less than 10% residue was left at 700°C in DGEBA/DDM.[5]

Regardless of the atmosphere used, the curves of the different heating rates were parallel for the first weight-loss step, and this implied a single decomposition mechanism in this part of the degradation. Ozawa's model provides a widely applicable method of analyzing thermogravimetric data, with which the random degradation of high polymers can also be treated.[24] Equation (4) is suitable for analyzing the thermal decomposition reaction, for which the conversion is defined as the weight-loss percentage and T is conversion-dependent. A plot of $\ln(\beta)$ verse $1/T$ (Fig.

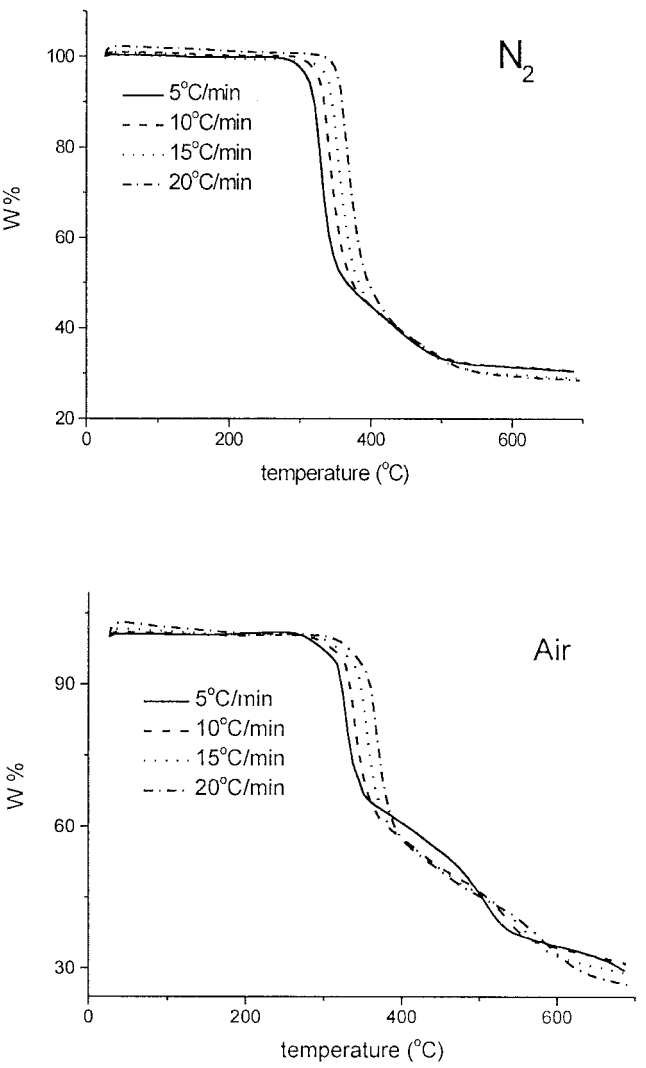

Figure 4 TGA spectra of DGEBA/BAPP at different heating rates.

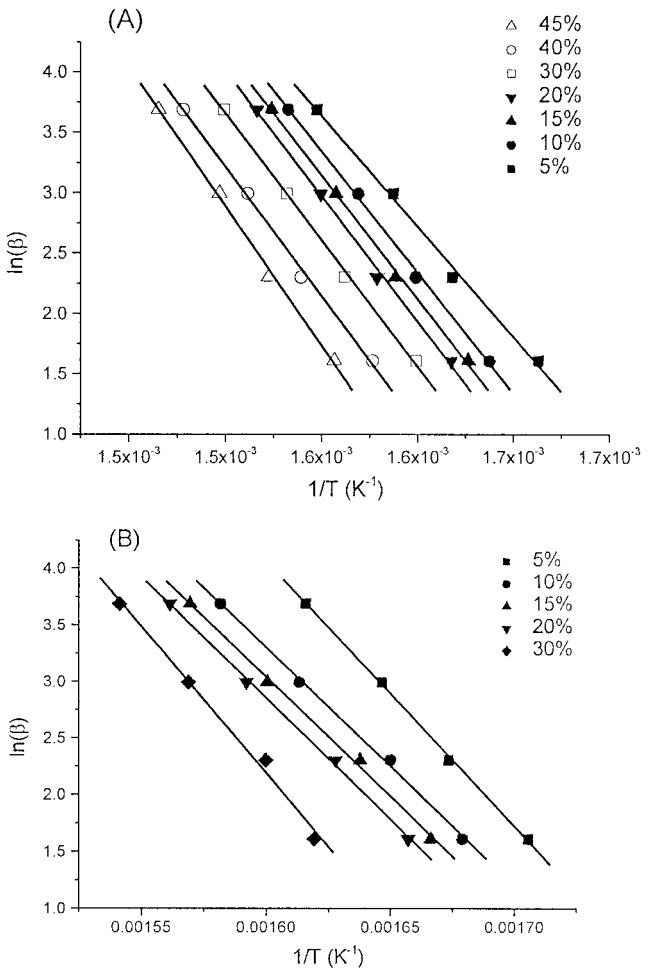

Figure 5 Dynamic kinetic analysis of the first degradation step of DGEBA/BAPP (A) in an N_2 atmosphere and (B) in an air atmosphere for different levels of weight loss.

5) demonstrates good linearity for the DGEBA/BAPP epoxy resin system. The activation energies for all the epoxy resin systems under different conversions were calculated from the slope and are shown in Figure 6. For the same degree of degradation, the activation energy in air was higher than that in N_2 in all cases. This means that DGEBA/BAPP was more stable in air than in N_2.

As shown in Figure 6, the activation energy increased gradually with increasing weight loss. In N_2, the activation energy could not be calculated after the weight loss reached 50%, defined as the critical weight loss, because the four TGA curves overlapped after this critical weight loss. In view of Ozawa's analysis, the activation energy in this case should be infinite and the weight loss should be zero. In fact, the weight loss slowed down dramatically, and the activation energy appeared to be too large to be calculated from the current range of heating rates. According to the condensed phase mechanism of phosphorus-containing flame retardants,[27] a char produced during decomposition improves the thermal stability and increases the decomposition activation energy. In an air atmosphere, this phenomenon appears at a low critical conversion (ca. 36%), and even the sample scanned at 5°C/min showed a lower weight loss from 400 to 500°C. This unusual result has also been reported elsewhere[28] for DGEBA cured with 1,4-bis(3-aminobenzoyloxy)-2-(6-oxido-6H-dibenz⟨c,e⟩⟨1,2⟩oxaphosphorin-6-yl)phenylene. It may be due to the reducing character of the phosphine oxide group and its reaction with oxygen. This reaction can lower the oxidation of the carbon to CO and CO_2, promote the charring process, and sup-

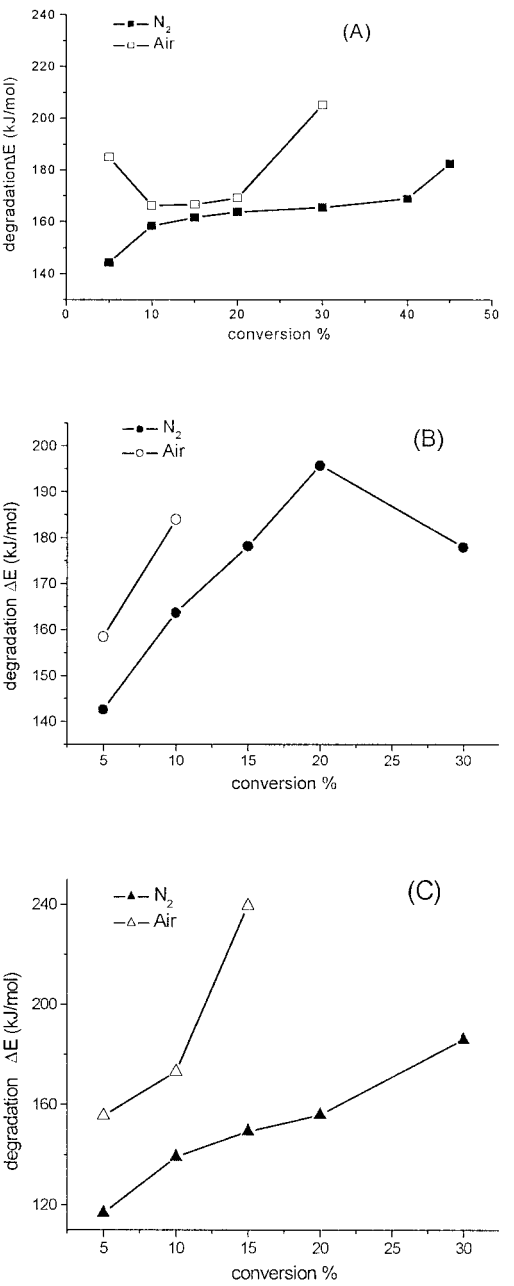

Figure 6 Degradation activation energies of (A) DGEBA/BAPP, (B) TGAP/BAPP, and (C) TGDDM/BAPP.

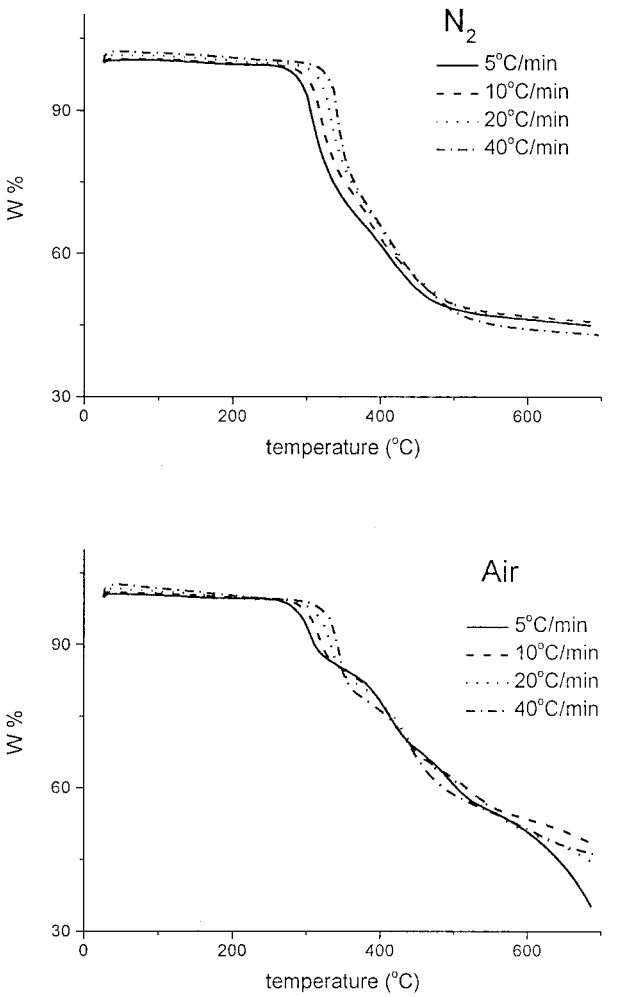

Figure 7 TGA spectra of TGAP/BAPP at different heating rates.

press the glow of charred residue.[27] The morphology of the final degradation product yielded further evidence; the char achieved in N_2 was loose and porous, whereas the char given in air was denser. The unusual behavior at the 5°C/min scanning rate could be explained by the long reaction time between the oxygen and phosphine oxide group and the higher yield of the phosphorus-rich thermally stable char. The thermal degradation behaviors of the TGAP/BAPP and TGDDM/BAPP systems were similar to that of DGEBA/BAPP, except for different critical weight-loss values, as shown in Figures 7 and 8. Their thermal degradation activation energies in the first weight-loss step in both N_2 and air atmospheres were calculated with Ozawa's method, and the values are given in Figure 6. The multistep degradation process in air was also found in the TGAP/BAPP and TGDDM/BAPP systems, and a relatively high char yield at 700°C resulted. Further isothermal TGA will help us to understand the underlying nature of the multistep degradation.

The char yields at 700°C in N_2 and air of DGEBA/BAPP were 31%; according to the proportional relationship between the char yield and limiting oxygen index (LOI), the high LOI and improved flame retardancy can be predicted rationally. Although the char yield at 700°C in N_2 was the same as that in air, the char yields at 500 and 600°C in N_2 were much lower than those in air. The further weight loss in an air atmosphere for temperatures greater than 500°C could be due to the oxidation of phosphorus-rich char. Thus, any method of enhancing the oxidation stability of the char should improve the flame retardancy.

CONCLUSIONS

A phosphorus-containing amine, BAPP, was synthesized successfully and characterized with FTIR spectrometry and NMR. BAPP exhibited reactivity similar to that of DDM but greater reactivity than DDS, as determined from the initial curing temperature and onset curing temperature shown in DSC scans and the chemical shift shown in ^1H NMR. The curing reaction

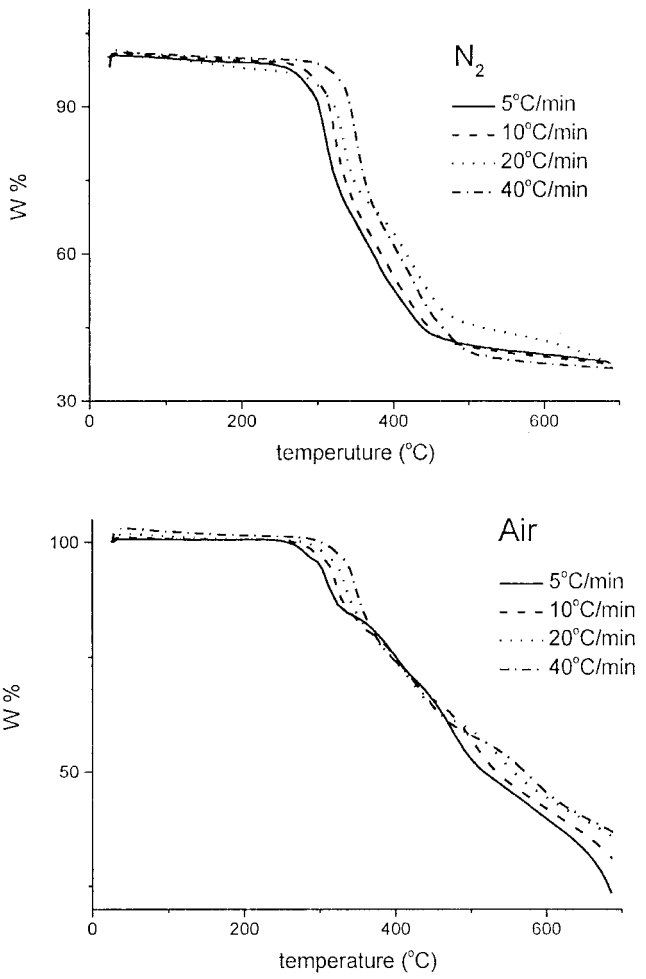

Figure 8 TGA spectra of TGDDM/BAPP at different heating rates.

activation energies of BAPP with DGEBA, TGAP, and TGDDM were calculated according to the Kissinger and Ozawa models and were found to be comparable to those of DDM but significantly lower than those of DDS. TGA of the BAPP cured epoxy resin systems in both nitrogen and air atmospheres showed multistep thermal degradation and high char yields, as expected for phosphorus-containing flame-retardant epoxy resins. The degradation activation energies of the first thermal weight-loss step calculated from the Ozawa method revealed that the cured systems were more stable in an air atmosphere than in a nitrogen one. This was found to be the case for all of the epoxy resin systems and was attributed to the ability of the phosphine group to react with oxygen, which promoted the formation of the char layer and thus increased thermal stability. The increased char yield of the BAPP hardener, compared with that of the DDM hardener, provided evidence of the likely improvement in the fire performance of these epoxy resin systems.

References

1. Hilado, C. J. Flammability Handbook for Plastics, 5th ed; Technomic: Lancaster, PA, 1998.
2. Zaikov, G. E.; Lomakin, S. M. J Appl Polym Sci 2002, 86, 2449.
3. Wu, C. S.; Liu, Y. L.; Chiu, Y. S. Polymer 2002, 43, 4277.
4. Chen, Y. W.; Lee, H. F.; Yuan, C. Y. J Polym Sci Part A: Polym Chem 2000, 38, 972.
5. Liu, Y. L.; Hsiue, G. H.; Chiu, Y. S. J Polym Sci Part A: Polym Chem 1997, 35, 565.
6. Wang, C. S.; Sieh, J. Y. Eur Polym J 2000, 36, 443.
7. Wang, C. S.; Sieh, J. Y. Polymer 1998, 39, 5819.
8. Lin, C. H.; Wang, C. S. Polymer 2001, 42, 1869.
9. Jeng, R. J.; Shau, S. M.; Lin, J. J.; Su, W. C.; Chiu, Y. S. Eur Polym J 2002, 38, 683.
10. Shau, M. D.; Wang, T. S. J Polym Sci Part A: Polym Chem 1996, 34, 387.
11. Wang, C. S.; Lin, C. H. J Polym Sci Part A: Polym Chem 1999, 37, 3903.
12. Liu, Y. L.; Hsiue, G. H.; Chiu, Y. S.; Jeng, R. J.; Perng, L. H. J Appl Polym Sci 1996, 61, 613.
13. Liu, Y. L.; Hsiue, G. H.; Chiu, Y. S.; Jeng, R. J. J Appl Polym Sci 1996, 61, 1789.
14. Shieh, J. Y.; Wang, C. S. J Appl Polym Sci 2000, 78, 1636.
15. Levchik, S. V.; Camino, G.; Luda, M. P.; Costa, L.; Muller, G.; Costes, B. Polym Degrad Stab 1998, 60, 169.
16. Levchiv, S. V.; Camino, G.; Costa, L.; Luda, M. P. Polym Degrad Stab 1996, 54, 317.
17. Liu, Y. L. Polymer 2001, 42, 3445.
18. Shieh, J. Y.; Wang, C. S. Polymer 2001, 42, 7617.
19. Jain, P.; Choudhary, V.; Varma, I. K. J Therm Anal Calorim 2002, 67, 761.
20. Liu, Y. L.; Hsiue, G. H.; Lee, R. H.; Chiu, Y. S. J Appl Polym Sci 1997, 63, 895.
21. Hsiue, G. H.; Liu, Y. L.; Tsiao, J. J Appl Polym Sci 2000, 78, 1.
22. Gunther, H. NMR Spectroscopy: Basic Principles, Concepts, and Applications in Chemistry, 2nd ed.; Wiley: New York, 1995.
23. Kissinger, H. E. Anal Chem 1957, 29, 1702.
24. Ozawa, T. Bull Chem Soc Jpn 1965, 38, 1881.
25. Barton, J. M. Makromol Chem 1973, 171, 247.
26. Apicella, A.; Nicolais, L.; Iannone, M.; Passerini, P. J Appl Polym Sci 1984, 29, 2083.
27. Toritzch, J. H. Prog Org Coat 1983, 11, 41.
28. Wang, C. S.; Lin, C. H. J Appl Polym Sci 1999, 74, 1635.